

See discussions, stats, and author profiles for this publication at: <https://www.researchgate.net/publication/11520327>

The Molecular Mechanism of Stabilization of Proteins by TMAO and Its Ability to Counteract the Effects of Urea

ARTICLE *in* JOURNAL OF THE AMERICAN CHEMICAL SOCIETY · MARCH 2002

Impact Factor: 12.11 · DOI: 10.1021/ja004206b · Source: PubMed

CITATIONS

251

READS

131

4 AUTHORS, INCLUDING:



Brian J Bennion

Lawrence Livermore National Laboratory

25 PUBLICATIONS 1,305 CITATIONS

SEE PROFILE



Valerie Daggett

University of Washington Seattle

223 PUBLICATIONS 12,608 CITATIONS

SEE PROFILE



Kenneth P Murphy

University of Iowa

48 PUBLICATIONS 3,672 CITATIONS

SEE PROFILE

The Molecular Mechanism of Stabilization of Proteins by TMAO and Its Ability to Counteract the Effects of Urea

Qin Zou,[†] Brian J. Bennion,[‡] Valerie Daggett,^{†,‡} and Kenneth P. Murphy^{*,†}

Contribution from the Department of Biochemistry, University of Iowa College of Medicine, Iowa City, Iowa 52242, and Department of Medicinal Chemistry, University of Washington, Seattle, Washington 98195-7610

Received December 7, 2000

Abstract: Trimethylamine *n*-oxide (TMAO) is a naturally occurring osmolyte that stabilizes proteins and offsets the destabilizing effects of urea. To investigate the molecular mechanism of these effects, we have studied the thermodynamics of interaction between TMAO and protein functional groups. The solubilities of a homologous series of cyclic dipeptides were measured by differential refractive index and the dissolution heats were determined calorimetrically as a function of TMAO concentration at 25 °C. The transfer free energy of the amide unit (–CONH–) from water to 1 M TMAO is large and positive, indicating an unfavorable interaction between the TMAO solution and the amide unit. This unfavorable interaction is enthalpic in origin. The interaction between TMAO and apolar groups is slightly favorable. The transfer free energy of apolar groups from water to TMAO consists of favorable enthalpic and unfavorable entropic contributions. This is in contrast to the contributions for the interaction between urea and apolar groups. Molecular dynamics simulations were performed to provide a structural framework for the interpretation of these results. The simulations show enhancement of water structure by TMAO in the form of a slight increase in the number of hydrogen bonds per water molecule, stronger water hydrogen bonds, and long-range spatial ordering of the solvent. These findings suggest that TMAO stabilizes proteins via enhancement of water structure, such that interactions with the amide unit are discouraged.

Introduction

Protein stability is the result of a balance between the intramolecular interactions of protein functional groups and their interactions with the solvent environment. Adding cosolvents into the protein solution can modify this balance. Cosolvents have been used widely to isolate, dissolve and stabilize proteins. They are also useful in studying protein folding and the interactions that stabilize protein structures.^{1–4} Cosolvents also find application in the pharmaceutical and biotechnology industries to dissolve and refold insoluble, recombinant proteins and to extend the shelf life of proteins. Recently, it has been found that some cosolvents, known as chemical chaperones, are able to correct protein-folding defects that are related to some diseases.^{5–7}

Naturally occurring osmolytes are cosolvents that are used to protect organisms from denaturation via environmental stress.

For example, trimethylamine-*N*-oxide (TMAO) accumulates in coelacanth and marine elasmobranchs to offset the deleterious effects of urea.⁸ Urea is also concentrated in these animals to balance osmotic pressure. TMAO belongs to the family of “counteracting” osmolytes⁹ that includes betaine and glycerophosphocholine, which are naturally accumulated in mammalian kidney.^{10–12} “Counteracting” osmolytes affect both protein stability and function, while “compatible” osmolytes,⁹ including sucrose and some amino acids, only affect protein stability.

The effect of TMAO on protein stability and enzyme activity has been widely studied. TMAO can increase the melting temperature as well as the unfolding free energy of proteins^{13–15} and offset the destabilizing effects of urea. TMAO can also restore enzyme activity that is lost upon urea treatment.^{16–18}

* Correspondence may be addressed either to Kenneth Murphy at Department of Biochemistry, University of Iowa College of Medicine, Iowa City, IA 52242; telephone: (319) 335-8910; fax: (319) 335-9570; e-mail: k-murphy@uiowa.edu; or to Valerie Daggett at Department of Medicinal Chemistry, University of Washington, Seattle, WA 98195-7610; telephone: (206) 685-7420; fax: (206) 685-3252; e-mail: daggett@u.washington.edu.

[†] University of Iowa College of Medicine.

[‡] University of Washington.

- (1) Fujita, Y.; Miyana, A.; Noda, Y. *Bull. Chem. Soc. Jpn.* **1979**, *52*, 3659–3662.
- (2) Velicelebi, G.; Sturtevant, J. M. *Biochemistry* **1979**, *18*, 1180–1186.
- (3) Fujita, Y.; Miyana, A.; Noda, Y. *Bull. Chem. Soc. Jpn.* **1983**, *56*, 233–237.
- (4) Fu, L.; Freire, E. *Proc. Natl. Acad. Sci. U.S.A.* **1992**, *89*, 9335–9338.

- (5) Brown, C. R.; Hong-Brown, L. Q.; Biwersi, J.; Verkman, A. S.; Welch, W. J. *Cell Stress Chaperones* **1996**, *1*, 117–125.
- (6) Brown, C. R.; Hong-Brown, L. Q.; Welch, W. J. *J. Clin. Invest.* **1997**, *99*, 1432–1444.
- (7) Tatzelt, J.; Prusiner, S. B.; Welch, W. J. *EMBO J* **1996**, *15*, 6363–6373.
- (8) Yancey, P. H.; Somero, G. N. *J. Exp. Zool.* **1980**, *212*, 205–213.
- (9) Yancey, P. H.; Clark, M. E.; Hand, S. C.; Bowlus, R. D.; Somero, G. N. *Science* **1982**, *217*, 1214–1222.
- (10) Bagnosco, S.; Balaban, R.; Fales, H. M.; Yang, Y.-M.; Burg, M. J. *Biol. Chem.* **1986**, *261*, 5872–5877.
- (11) Garcia-Perez, A.; Burg, M. B. *Hypertension* **1990**, *16*, 595–602.
- (12) Nakanishi, T.; Uyama, O.; Nakahama, H.; Takamitsu, Y.; Sugita, M. *Am. J. Physiol.* **1993**, *264*, F472–F479.
- (13) Yancey, P. H.; Somero, G. N. *Biochem. J.* **1979**, *183*, 317–323.
- (14) Arakawa, T.; Timasheff, S. N. *Biophys. J.* **1985**, *47*, 411–414.
- (15) Lin, T. Y.; Timasheff, S. N. *Biochemistry* **1994**, *33*, 12695–12701.
- (16) Mashino, T.; Fridovich, I. *Arch. Biochem. Biophys.* **1987**, *258*, 356–360.
- (17) Baskakov, I.; Bolen, D. W. *Biophys. J.* **1998**, *74*, 2658–2665.
- (18) Baskakov, I.; Wang, A.; Bolen, D. W. *Biophys. J.* **1998**, *74*, 2666–2673.

To provide more chemical insight into TMAO's role in protein stabilization and in counteracting the effect of urea, Wang and Bolen¹⁹ investigated the transfer free energies of model compounds. They found that the unfavorable interaction between TMAO and the peptide backbone makes the dominant contribution to stabilization. However, to reveal the molecular mechanism by which TMAO stabilizes proteins, more detailed thermodynamics about the molecular interaction between TMAO and protein functional groups are needed. Molecular dynamics simulations are also an effective tool for delineating the interactions involved in complex thermodynamic systems. Unfortunately, earlier simulations and ab initio calculations of TMAO²⁰ did not include any protein functional groups and only focused on water–TMAO interactions.

Previously we investigated the dissolution energetics of a homologous series of cyclic dipeptides to study the molecular interactions between urea and protein functional groups.²¹ The interaction of these molecules has been shown to closely mimic the energetics of protein folding.^{21–23,36} Here, we use the same approach to investigate the energetics of the interactions between TMAO and protein functional groups. Hence, our system is a ternary component system (protein functional groups, water, and TMAO) containing various weak interactions. In addition, we combine these experiments with molecular dynamics (MD) simulations to obtain a framework for understanding these weak interactions and to investigate the molecular mechanism by which TMAO stabilizes proteins and counteracts the effects of urea.

Materials and Methods

Calorimetry Studies. Cyclo(Gly-Gly) was obtained from Sigma (St. Louis, MO). Cyclo(Ala-Gly) and cyclo(Ala-Ala) were obtained from Bachem Bioscience Inc. (Philadelphia, PA). These dipeptides are designated as c(GG), c(AG), and c(AA), respectively, and were used without further purification. Trimethylamine-*N*-oxide was obtained from Sigma (St. Louis, MO) and the concentration of TMAO solutions was measured by refractive index based on an empirical equation.¹⁹ More hydrophobic cyclic dipeptides, such as cyclo(Leu-Ala), could not be used here because of their very low solubilities in TMAO solution.

The solubilities of the cyclic dipeptides in TMAO solution were determined at 25 °C by differential refractive index measurement as

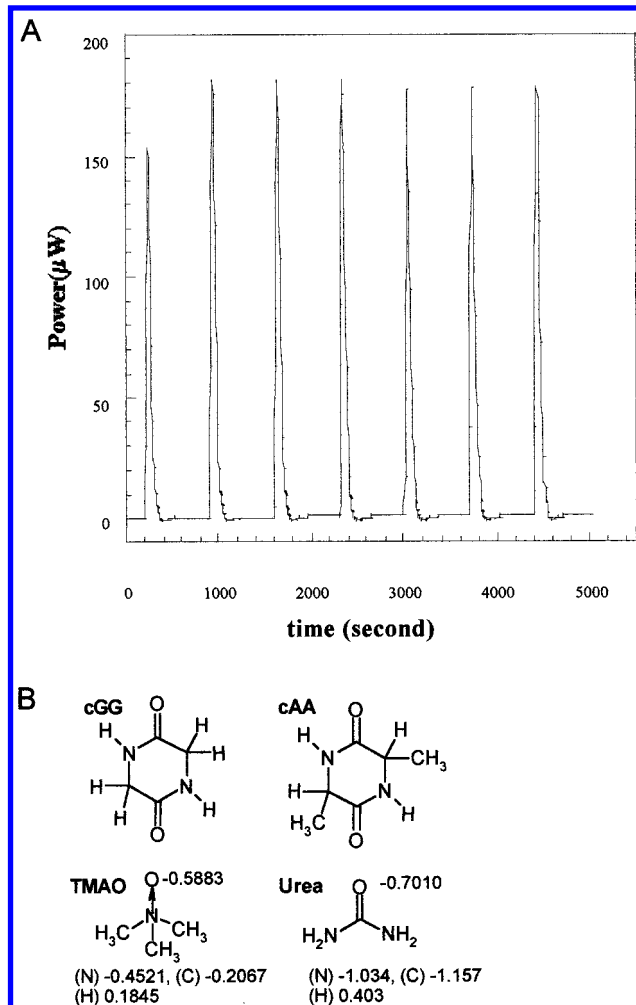


Figure 1. (A) Typical PEPC experiment on cAA in 0.5M TMAO at 25 °C. The injection volume is 5 mL for each peak. The average heat was obtained from the middle five peaks. (B) Structures and partial charges for each of the solute molecules used in the simulations. Other parameters are the same as those described elsewhere.^{26,27}

previously described.²² The dissolution free energy (ΔG°) of these dipeptides in TMAO solution is given as:

$$\Delta G^\circ = -RT \ln K_s \quad (1)$$

where K_s is the solubility, R is the gas constant, and T is the absolute temperature.

The dissolution heat of the cyclic dipeptides in TMAO solutions was measured at 25 °C by phase equilibrium perturbation calorimetry (PEPC) as previously described,^{22,23} using a model 4200 isothermal titration calorimeter (Calorimetry Science Corporation, Spanish Fork, UT). The dissolution enthalpy (ΔH°) is related to the heat of an injection, q , as:

$$\Delta H^\circ = \frac{q}{vK_s} \quad (2)$$

where v is the volume of solvent that is injected into the solution. A typical PEPC experiment is shown in Figure 1. Each peak results from one injection of the solvent and the area under the peak is the heat for that injection. The middle five peaks were used in calculating ΔH° .

Molecular Dynamics Simulations. The molecular dynamics methods as implemented within ENCAD,²⁴ protocols,²⁵ and potential function^{26,27} are described in detail elsewhere. Water molecules were added around the solute molecule, filling a rectangular box at least

- (19) Wang, A.; Bolen, D. W. *Biochemistry* **1997**, *36*, 9101–9108.
- (20) Noto, R.; Martorana, V.; Emanuele, A.; Fornili, S. L. *J. Chem. Soc., Faraday Trans.* **1995**, *91*, 3803–3808.
- (21) Zou, Q.; Habermann-Rottinghaus, S. M.; Murphy, K. P. *Proteins* **1998**, *31*, 107–115.
- (22) Murphy, K. P.; Gill, S. J. *Thermochim. Acta* **1990**, *172*, 11–20.
- (23) Murphy, K. P.; Gill, S. J. *J. Chem. Thermodyn.* **1989**, *21*, 903–913.
- (24) Levitt, M. *ENCAD*; Stanford University and Yeda: Stanford, CA, 1990.
- (25) Daggett, V.; Levitt, M. *J. Mol. Biol.* **1992**, *223*, 1121–1138.
- (26) Levitt, M.; Hirshberg, M.; Sharon, R.; Daggett, V. *Comp. Phys. Commun.* **1995**, *91*, 215–231.
- (27) Levitt, M.; Hirshberg, M.; Sharon, R.; Laidig, K. E.; Daggett, V. *J. Phys. Chem.* **1997**, *101*, 5051–5061.
- (28) Weast, R.; Astle, M. J. *Handbook of Chemistry and Physics*; CRC Press: Boca Raton, 1980.
- (29) Withers, P. C.; Morrison, G.; Hefter, G. T.; Pang, T. S. *J. Exp. Biol.* **1994**, *188*, 175–189.
- (30) Hariharan, P. C.; Pople, J. A. *Theor. Chim. Acta* **1973**, *28*, 213–222.
- (31) Krishnan, R.; Binkley, J. S.; Seeger, R.; Pople, J. A. *J. Chem. Phys.* **1980**, *72*, 650–654.
- (32) Frisch, M. J.; Pople, J. A.; Binkley, J. S. *J. Chem. Phys.* **1984**, *80*, 3265–3269.
- (33) Schmidt, M. W.; Baldridge, K. K.; Boatz, J. A.; Elbert, S. T.; Gordon, M. S.; Jensen, J. H.; Koseki, S.; Matsunaga, N.; Nguyen, K. A.; Su, S.; Windus, T. L.; Dupuis, M.; Montgomery, J. A., Jr. *J. Comput. Chemistry* **1993**, *14*, 1347–1363.
- (34) Spackman, M. A. *J. Comput. Chem.* **1996**, *17*, 1–18.
- (35) Gill, S.; Wadso, I. *Proc. Natl. Acad. Sci. U.S.A.* **1976**, *73*, 2955–2958.
- (36) Murphy, K. P.; Freire, E. *Adv. Protein Chem.* **1992**, *43*, 313–361.

Table 1. Properties of the Systems Simulated

system	box volume (Å ³)	no. cosolvent	no. waters	mass of cosolvent (g)	mass of water (g)	total system mass (g)	solution density (g/mL) ^a	
							MD	expt
1 M urea	6644.7	4	211	240.224	3801.165	4041.389	1.014	1.015
2 M urea	6762.0	8	206	480.449	3711.090	4191.539	1.034	1.031
3 M urea	7744.8	12	202	720.673	3639.030	4359.703	0.938	1.046
4 M urea	7267.6	17	197	1020.954	3548.955	4569.909	1.048	1.061
1 M TMAO	6821.5	4	211	300.461	3801.165	4101.626	1.002	1.000
2 M TMAO	7241.8	8	206	600.922	3711.090	4312.012	0.993	1.004
3 M TMAO	7714.2	14	201	1051.613	3621.015	4672.628	1.009	1.009
4 M TMAO	8252.5	21	193	1577.419	3476.895	5054.314	1.020	1.016
cAA	8279.3	0	268	0.000	4828.020	4828.020	0.996	0.997
1 M TMAO	8499.6	5	255	375.550	4593.825	4969.375	0.998	1.000
1 M urea	8493.4	5	263	300.280	4737.945	5038.225	1.0130	1.015
cGG	7542.4	0	245	0.000	4413.675	4413.675	0.997	0.997
1 M TMAO	7752.2	4	234	300.440	4215.510	4515.950	0.991	1.000
1 M urea	7737.4	4	241	240.224	4341.615	4581.839	1.007	1.015

^a The solvent density in the MD simulations was calculated just for the solution, i.e., the solute volume was subtracted from the system volume. Experimental urea and water densities taken from the CRC.²⁹ Experimental TMAO densities from Auton and Bolen (personal communication) for the dihydrate, TMAO·2H₂O.

8 Å from any individual solute atom. A nonbonded cutoff of 8 Å with smooth, force-shifted truncation was used.²⁶ The density of the solvent was set to the experimental value for the solution and temperature of interest by adjusting the volume of the box. The experimental densities for solutions at 25 °C were used: pure water (0.9970 g/mL),²⁸ 1 M urea (1.0139 g/mL),²⁸ and 1 M TMAO (0.9996 g/mL) (Mathew Auton and Wayne Bolen, personal communication) (and see Table 1). Periodic-boundary conditions with the minimum image convention were employed. Solvent molecules were explicitly present, eliminating the need for a macroscopic dielectric constant.

The intra- and intermolecular parameters for urea were taken directly from the ENCAD parameter set.²⁶ The atomic partial charges used in this study were determined from ab initio molecular orbital calculations. The molecular charge distribution was determined using the balanced, polarized, and diffuse basis set 6-311++G**.^{30–32} The SCF calculations were limited to the HF level and done using the GAMESS program suite.³³ Atomic point charges were fit so as to yield the molecular electrostatic potential using the GEODESIC algorithm,³⁴ as implemented within GAMESS.

The three-dimensional structure and atomic partial charges for TMAO were initially taken from Noto et al.²⁰ and subsequently modified. The atomic partial charges as originally reported did not give a net neutral molecule (Figure 1); slight modifications were made to ensure neutrality. The three-dimensional structure was optimized in vacuo and converged with 93 steps of conjugate gradient minimization. Models for cyclic dialanine (cAA) and diglycine (cGG) were prepared using the ENCAD parameter set, with modification to the peptide bond conformation. The original peptide parameters were modified to make the cis conformation (omega torsion angle set to 180° instead of 0°).²⁶ The resulting structures of cAA and cGG converged at 108 and 250 steps of minimization, respectively.

Single solute trajectories were prepared by solvating the solute with water molecules at the appropriate density, as described above.^{28,29} A variety of steps were performed to prepare the systems for MD. First, solvent alone was minimized (solute position and energy remained constant) for 1500 steps followed by 15 000 steps of MD. Next, another 1500 steps of minimization were performed on the solvent. The solute was then subjected to 500 to 1500 steps of CG minimization depending on convergence of the individual solute. Finally, the whole system was minimized for 1500 steps. Molecular dynamics simulations were performed for 4 ns at 25 °C using the microcanonical ensemble with non-bonded interactions updated every other step of dynamics (every 4 fs).

In simulations where cosolvent was present, an initial water box was constructed. Then a TMAO or urea mole fraction of 0.019 (1 M solutions) was obtained by randomly replacing 4–5 water molecules by cosolvent. The initial box contained water with a low density to

Table 2. Contributions of Protein Functional Groups to the Transfer Energetics in 1 M TMAO and 1 M Urea

	1 M TMAO ^a		1 M urea ^b	
	one amide unit –CONH–	one apolar hydrogen	one amide unit –CONH–	one apolar hydrogen
ΔG_{tr} (J/mol)	462 ± 60	–15 ± 18	–54 ± 19	–16 ± 4
ΔH_{tr} (J/mol)	2113 ± 126	–428 ± 33	–727 ± 75	75 ± 16
ΔS_{tr} (J/mol·K)	5.5 ± 0.5	–1.4 ± 0.1	–2.3 ± 0.2	0.30 ± 0.04

^a Errors were propagated using KaleidaGraph. ^b Data from ref 21.

obtain the proper, experimental density for the final water-cosolvent system. System densities were verified by summing the mass of the solvent atoms and dividing by the box volume (excluding the solute volume) (Table 1). The densities could not change over the course of MD because of the use of the NVE ensemble. The densities in the simulations were within experimental error. Details regarding the composition of the systems simulated and their densities are summarized in Table 1. Trajectories were then prepared for MD by minimizing the entire system (solute, solvent, and cosolvent) for 2000 steps. Next, MD was performed for 4000 steps followed by a second cycle of minimization for 2000 steps. The final cycle included 10 000 steps of MD, followed by 2000 steps of minimization. MD simulations were then performed for 4 ns at 25 °C, as described above. Structures were saved every 0.2 ps for analysis, resulting in 20 000 for each simulation.

Results

Calorimetry Studies. Group Contributions to the Transfer Free Energy from Water to TMAO. Figure 2 shows the ΔG° of dissolution as a function of TMAO concentration for the three cyclic dipeptides (cGG, cAA, cAG) at 25 °C. ΔG° increases linearly (i.e., becomes more unfavorable) with increasing TMAO concentration in all cases. The slopes of the fitted lines in Figure 2 are the transfer free energies (ΔG_{tr}) for these compounds from water to 1 M TMAO. ΔG_{tr} changes with the size of the aliphatic side chain, as is seen in the plot of the slope versus the number of apolar hydrogens (N_{aH} , Figure 3). Apolar hydrogens are defined as hydrogens bonded to carbon and are related to the hydrophobic surface area of the peptides.^{35,36} Assuming group additivity, a linear regression line can be fitted to the data (see Figure 3), and the group contributions to ΔG_{tr} can be determined from the intercept and the slope. The intercept in Figure 3 is the transfer free energy for the two amide units (–CONH–) and the slope is for one apolar hydrogen. As shown in Table 2,

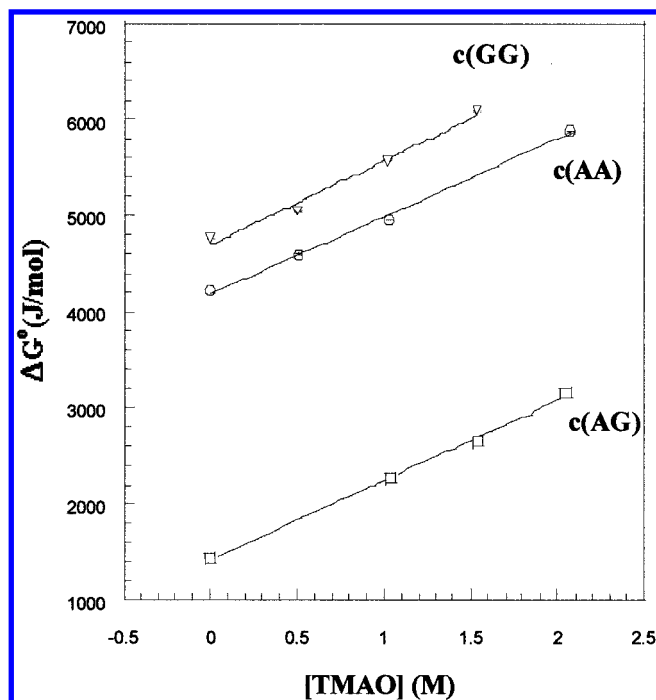


Figure 2. The dissolution free energy (ΔG°) at 25 °C as a function of TMAO concentration for all three cyclic dipeptides. The slope of the fitted line represents the transfer free energy of the peptides from water to 1 M TMAO. The errors bars show the experimental uncertainties. The lines are linear fits for all three dipeptides by KaleidaGraph.

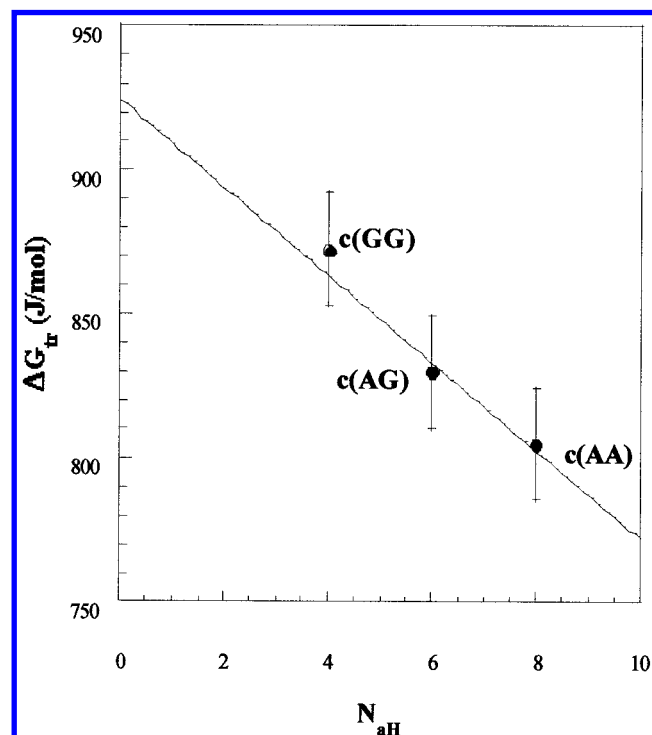


Figure 3. The transfer free energy (ΔG_{tr}) in 1 M TMAO as a function of the number of apolar hydrogens (N_{aH}). Group contributions are obtained from the y-intercept and the slope of the fitted line. The errors are from the linear regression in Figure 2.

ΔG_{tr} for the amide unit is quite large and positive with a value of 462 ± 60 J/mol. ΔG_{tr} for one apolar hydrogen is small and negative, with a value of -15 ± 18 J/mol. Consequently, it is unfavorable to transfer one amide unit from water to TMAO but slightly favorable to transfer apolar groups.

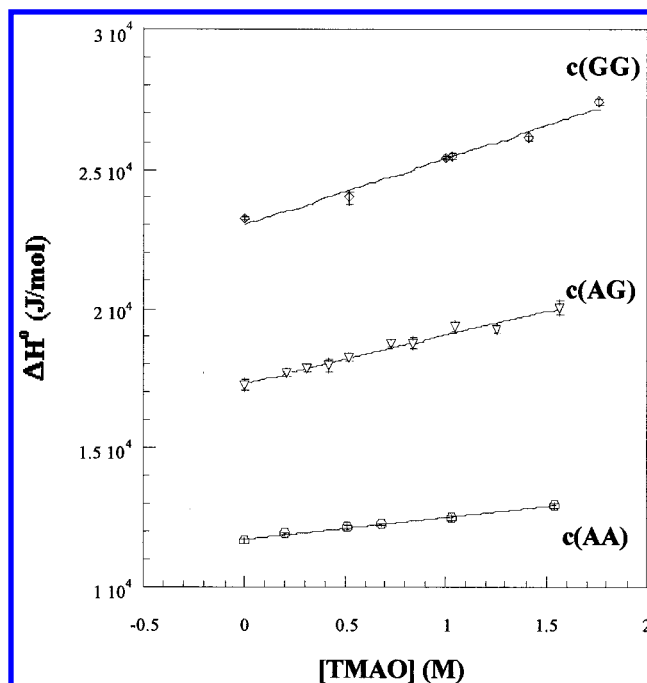


Figure 4. The dissolution enthalpy (ΔH°) at 25 °C as a linear function of TMAO concentration for the three cyclic dipeptides. The lines are linear regression fits by KaleidaGraph. The slope represents the transfer enthalpy (ΔH_{tr}) for the peptides from water to 1 M TMAO. The error bars are experimental uncertainties.

Enthalpic and Entropic Contributions to the Transfer from Water to TMAO. The dissolution enthalpy (ΔH°) for the three dipeptides at 25 °C in TMAO aqueous solution was also determined. The dissolution of all three dipeptides in TMAO solution is endothermic and ΔH° increases linearly with increasing TMAO concentration (Figure 4). As with ΔG_{tr} , the slopes of the linear regression lines are the transfer enthalpies (ΔH_{tr}) from water to 1 M TMAO and can be plotted versus N_{aH} (Figure 5). Again, the intercept of the linear regression line is the transfer enthalpy for the two amide units and the slope is for one apolar hydrogen. As summarized in Table 2, ΔH_{tr} for one amide unit is 2.0 ± 0.1 kJ/mol, while that for one apolar hydrogen is -0.43 ± 0.03 kJ/mol. Therefore, the enthalpic contribution to ΔG_{tr} for the amide unit is very unfavorable and that for the apolar group is favorable.

The transfer entropy (ΔS_{tr}) can be calculated from ΔH_{tr} and ΔG_{tr} for the amide unit and the apolar groups, using the standard equation:

$$\Delta G^\circ = \Delta H^\circ - T\Delta S^\circ \quad (3)$$

ΔS_{tr} for one amide unit and one apolar hydrogen are 5.5 ± 0.5 J/(mol·K) and -1.4 ± 0.1 J/(mol·K), respectively (Table 2). Thus, the entropic contribution for transfer of the amide unit from water to 1 M TMAO is favorable, while the entropy for transfer of the apolar groups is unfavorable. In summary, the calorimetric results indicate that the unfavorable enthalpy outweighs the favorable entropy to yield an unfavorable transfer free energy for the amide unit to 1 M TMAO. The slightly favorable transfer free energy for the apolar groups is enthalpically driven.

Molecular Dynamics Simulations

A variety of simulations were performed to investigate the interactions between urea, TMAO, and water with cAA and

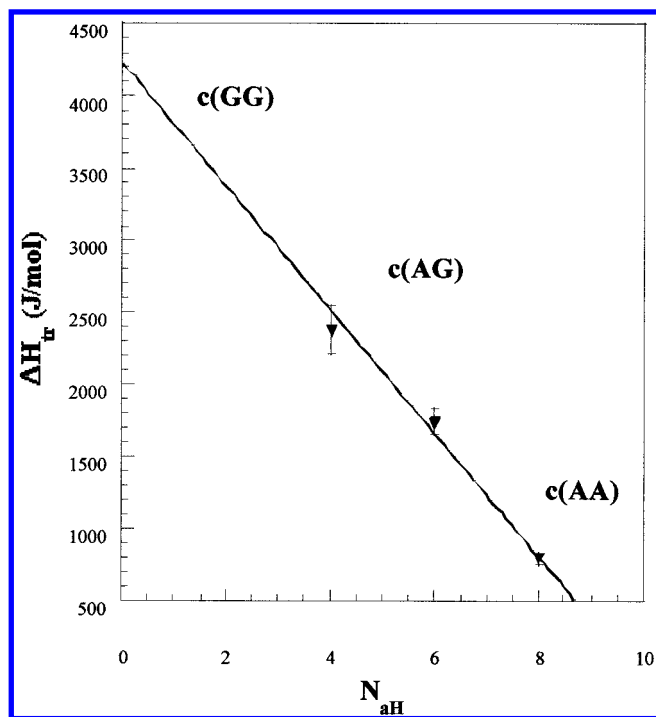


Figure 5. The transfer enthalpy (ΔH_{tr}) in 1 M TMAO as a function of the number of apolar hydrogens (N_{ah}). Group contributions are obtained from the y-intercept and the slope of the fitted line. The error bar is the fitted error from Figure 4.

cGG (Tables 3, 4, and 5). In addition, the effects of TMAO and urea on water structure and dynamics were investigated in the absence of peptide.

Solution Structure and Dynamics. The O–O water radial distribution functions for pure water, 1 M urea, and 1 M TMAO are given in Figure 6. Such plots are used to assess the structure of liquids. The water structure is largely unaffected upon addition of urea. In contrast, addition of TMAO leads to an increase in the first peak, which corresponds to a higher population of tetrahedrally oriented waters, or in other words, an increase in water structure. Water diffusion decreases in the presence of all solutes in the simulations with the exception of cAA in water or 1 M urea (Table 3). The reduction was most pronounced in simulations containing 1 M TMAO. A reduction in water diffusion of 30% by 1 M TMAO has been observed experimentally,³⁷ which translates to 0.17 Å²/ps given the experimental and simulated values for pure water 0.24 and 0.23 Å²/ps, respectively (Table 3). The simulations are in good agreement: the self-diffusion coefficient of water in 1 M TMAO solutions converged to 0.17 Å²/ps (Table 3).

Ordering of Water around Solutes: Angular Orientations. Direct interactions between solutes and cosolvents (TMAO and urea) are reflected in the number of heavy atom contacts between them (two aliphatic carbon atoms within 5.4 Å or distances involving polar heavy atoms within 4.6 Å). The number of contacts between solute and cosolvent is low for all solutes (Table 4). Nonetheless, there is a trend toward less direct solute–cosolvent interactions in TMAO compared with urea. Since direct interactions between cGG and cAA and TMAO and urea are minimal at these low concentrations, the possibility of indirect effects on water by cosolvent were considered.

Table 3. Properties of the Water in Various Solutions and Water–Solute and Water–Cosolvent Interactions^a

system	H ₂ O (Å ² /ps) ^b	HB per water ^c		no. solute– H ₂ O HB	HB lifetimes (ps)	
		hydration shell, ≤3 Å	bulk, >3 Å		H ₂ O– solute	H ₂ O– cosolvent
1 H ₂ O in H ₂ O	0.23	3.32	3.32	3.32	0.98	
1 H ₂ O in 1 M TMAO	0.17	3.38	3.34	3.33	1.02	7.47
1 H ₂ O in 1 M Urea	0.22	3.35	3.30	3.24	0.92	0.66
1 cGG in water	0.22	3.27	3.32	3.51	0.58	
1 cGG in 1 M TMAO	0.18	3.26	3.34	3.50	0.60	7.71
1 cGG in 1 M Urea	0.22	3.30	3.33	3.37	0.58	0.67
1 cAA in water	0.26	3.22	3.28	3.64	0.63	
1 cAA in 1 M TMAO	0.18	3.25	3.34	3.42	0.64	7.76
1 cAA in 1 M Urea	0.25	3.18	3.25	3.35	0.61	0.65

^a Simulations were performed for 4 ns, and the averages were taken over the last 2 ns (10 000 structures). ^b The average diffusion constant of water. The standard deviations of the diffusion constants ranged from 0.001 to 0.003 Å²/ps. ^c The average number of hydrogen bonds (donor–acceptor distance < 2.6 Å and a donor–H–acceptor angle within 35° of linearity) per water molecule. Errors of the mean at the 99.9% confidence interval were 0.003–0.009; therefore we consider the uncertainty to be ±0.01 hydrogen bonds per water molecule.

Table 4. Solute–Cosolvent Contacts for Single Molecule Solutes in 1 M TMAO or 1 M Urea^a

solute	no. solute–solvent contacts		no. solute–cosolvent contacts	
	pure water		1 M TMAO	1 M urea
water	12		0.34	0.35
TMAO	25		0.15	0.60
urea	20		0.28	0.44
cAA	30		1.10	1.10
cGG	24		0.72	0.88

^a Simulations were performed for 4 ns and averages taken over the last 2 ns of each simulation (10 000 structures). Heavy atom contacts are defined as two aliphatic carbon atoms within 5.4 Å and distances involving polar heavy atoms within 4.6 Å.

The effect of urea and TMAO on the orientation of water was investigated for simulations of pure water, 1 M TMAO, and 1 M urea. The orientation of water around the oxygen of the cosolvents was measured by an angle defined by two vectors. The first vector connects the solute oxygen to the water oxygen, and the second bisects the water hydrogen atoms in the plane of the water molecule (Figure 7A). Similarly, the water structure around the methyl groups of TMAO and NH₂ groups of urea were evaluated (Figure 7B).

With respect to orientation around the oxygens, all three simulations have a maximum at a radius of 2.5–3.0 Å with an angle of 35°; however, as the distance from the solute oxygen atom increases, the angular maxima diverge (Figure 7A). In the urea simulation, as the radius approaches 4 Å, the angular orientation is somewhat similar to that of water (~120°). In contrast, the water remains constrained to angles less than ~115° until a distance of 8 Å in the presence of TMAO. TMAO and urea share placement of one maximum near 5 Å, where water orients itself with angles between 30 and 50°, and the peak is 5% higher for TMAO. TMAO also has a maximum approaching 6 Å, where angles are restricted to about 105° (Figure 7A).

The waters are also restricted around the NH₂ groups of urea, with hydrogen bonding at approximately 140° (Figure 7B). Over 3 Å, the distribution broadens and the ordering drops off at 5 Å. The ordering of water imposed by the methyl groups of TMAO is more diffuse at shorter distances, but it extends to almost 6 Å. The presence of TMAO leads to greater spatial

(37) Clark, M. E.; Burnell, E. E.; Chapman, N. R.; Hinke, J. A. *Biophys. J.* **1982**, *39*, 289–299.

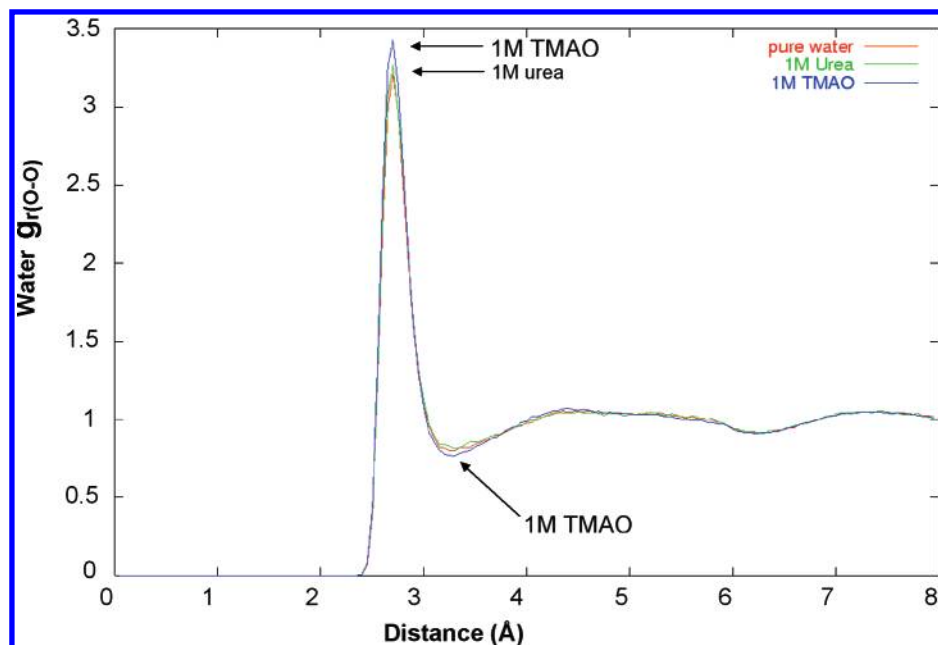


Figure 6. Water O–O radial distribution functions for pure water (red), 1 M TMAO (blue), and 1 M urea (green) simulations.

Table 5. Properties of 1–4 M Solutions of Urea and TMAO

solution	mol fraction	no. cosolvent molecules	no. waters	% H ₂ O under the influence of cosolvent
1 M urea	0.019	4	211	36
2 M urea	0.038	8	206	59
3 M urea	0.058	12	202	65
4 M urea	0.080	17	197	76
1 M TMAO	0.019	4	211	54
2 M TMAO	0.0422	8	206	86
3 M TMAO	0.0693	14	201	98
4 M TMAO	0.1018	21	193	9

^a Influenced water is defined as all water molecules within a 5.7 Å radius of a TMAO or 5.2 Å radius of a urea cosolvent molecule. These radii were chosen on the basis of the molecule's spatial influence on the angular orientation of water in Figure 6. Comparable results are obtained when a 5.7 or 5.2 Å cutoff was used for both TMAO and urea; TMAO still influenced more water molecules than urea. Values are averages from the last 2 ns (10 000 structures) of 4 ns trajectories.

and long-range order than urea (Figure 7B). Such TMAO-induced ordering of water was also observed in the cAA simulations. For example, water was more spatially constrained around the methyl groups of cAA in 1 M TMAO than in pure water or 1 M urea (Figure 7C).

Also shown in Figure 7 is the distance at which the influence of the solute on surrounding water begins to diminish. The radius of influence around the oxygen of TMAO extends much farther than the oxygens of water and urea. Also, due to TMAO's spatial influence and ability to closely coordinate water (Figure 8 and Table 5), a greater percentage of waters are in close proximity to TMAO compared with urea. For example, 54% of the waters are within the spatially affected sphere of influence of TMAO (5.7 Å, see Figure 7B) in the 1 M TMAO simulation, while the value is only 36% in 1 M urea (5.2 Å, Figure 7B and Table 5). The differences are even more striking for higher concentrations: the values are 86 and 59% for 2 M TMAO and urea, respectively; 4 M urea is necessary to yield a value approaching that of 2 M TMAO (Table 5).

Hydrogen-Bonding Properties of Solutions. Water hydrogen bonding is sensitive to the nature of the cosolvents. As a

result, hydrogen-bonding properties were determined and divided into two areas, structure and dynamics. Hydrogen bonds are defined as a hydrogen atom within 2.6 Å of an acceptor atom with an acceptor–H–donor angle less than 35° from linearity. With respect to structure, it is apparent that even liquid water does not completely hydrogen bond with itself (average hydrogen bonds per water = 3.32), as expected for a dynamic liquid (Table 3). On average, TMAO does not appear to disrupt the hydrogen bonding of the solvent, and, in fact, the number of hydrogen bonds per water tends to increase slightly in 1 M TMAO (Table 3). TMAO orders the nearby water, which is shown for a hydration layer around TMAO in Figure 8. In contrast, in 1 M urea the average number of hydrogen bonds per water molecule decreases slightly in most cases.

In simulations of the cyclic dipeptides in 1 M TMAO solutions, little TMAO is found in direct contact with the solute and therefore little hydrogen bonding occurs between the cosolvent and solute (Table 4, Figure 9). TMAO cosolvent molecules transiently hydrogen bond to cGG with a lifetime of 0.5 ps. However, no peptide hydrogen bonding was observed between cAA and TMAO (Figure 9). In all cases, upon addition of peptide solute to water, the hydrogen bonding in the hydration shell was compromised somewhat (Table 3).

The effect of TMAO is not limited to an increase in the average number of hydrogen bonds per water. TMAO also increases the strength of those hydrogen bonds. The distribution of water hydrogen bond lengths shifts to shorter distances (<1.8 Å) in 1 M TMAO with an increase of 43 such hydrogen bonds compared with those in pure water (Figure 10). In contrast, there is a loss of 23 tight hydrogen bonds upon the addition of 1 M urea.

Hydrogen bond lifetimes were calculated to address the stability of hydrogen bonds in various environments, with the behavior of pure water as our reference (the average hydrogen bond lifetime in pure water is 1.0 ps). Overall, the average water–water hydrogen-bonding lifetime is ~1.1 ps in the presence of cosolvents and solutes, and it increases slightly to 1.2 ps in 1 M TMAO simulations. On the other hand, the

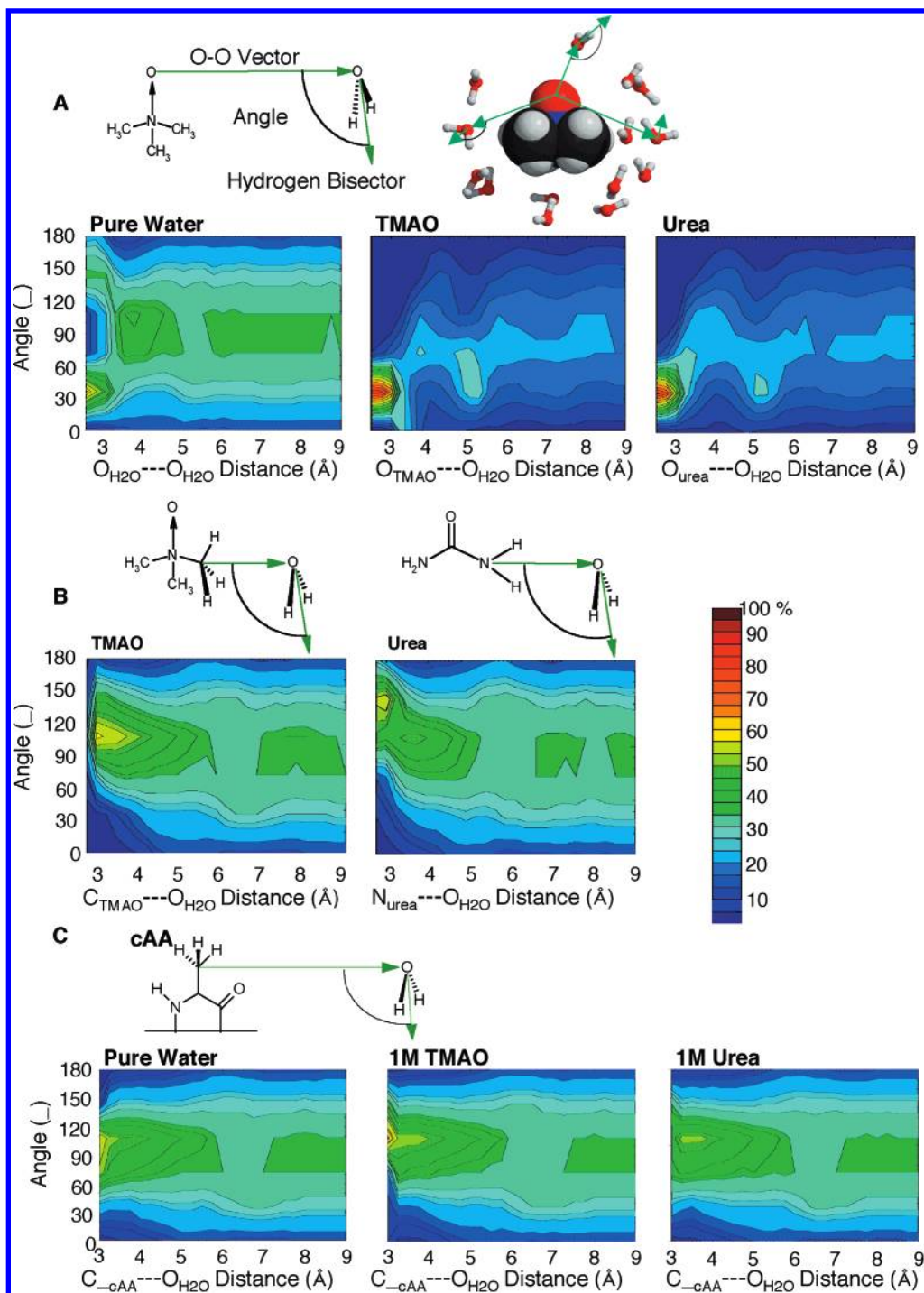


Figure 7. (A) Angular orientation of water molecules with respect to solute oxygen atoms. Orientational populations are presented as a contour map where each contour level corresponds to a 5% increase in the number of water molecules for each distance and angle. For each distance bin (27 0.5 Å bins), the angular populations sum to 100%. The color bar on the right relates the populations to the contour color. The distance between the main-chain oxygen of the solute to the oxygen atom of a water molecule is given on the *x*-axis. The *y*-axis represents the angle formed between solute and water from 0 to 180° as function of distance. Data are shown for pure water, 1 TMAO in water, and 1 urea in water. All points are averaged over the last 2 ns (10 000 structures); contour changes are significant at the 99.9% confidence interval. (B) Angular orientations of solvent water molecules with respect to the methyl groups of TMAO and the amide groups of urea. The distance between the main-chain carbon (TMAO, left) and nitrogen (urea, right) to the oxygen atom of water is given on the *x*-axis. The *y*-axis represents the angle formed between solute and water from 0 to 180° as function of distance. (C) Angular orientations of solvent water molecules with respect to the methyl groups of cAA, in pure water (left), 1 M TMAO (center) and 1 M urea (right). The distance between the C_{CAA} carbon (cAA) to the oxygen atom of water is given on the *x*-axis. The *y*-axis represents the angle formed between solute and water from 0 to 180° as function of distance.

average lifetimes of water–TMAO hydrogen bonds are over 7 ps (Table 3). Hydrogen-bonding lifetimes for water hydrogen bonding to urea are ~35% less than the water–water lifetimes (Table 3). Thus, water–water hydrogen bond lifetimes

are barely perturbed by the solutes and cosolvents, the hydrogen bond lifetimes for urea–water are shorter than water–water hydrogen bonds, and they are long-lived between water and TMAO.

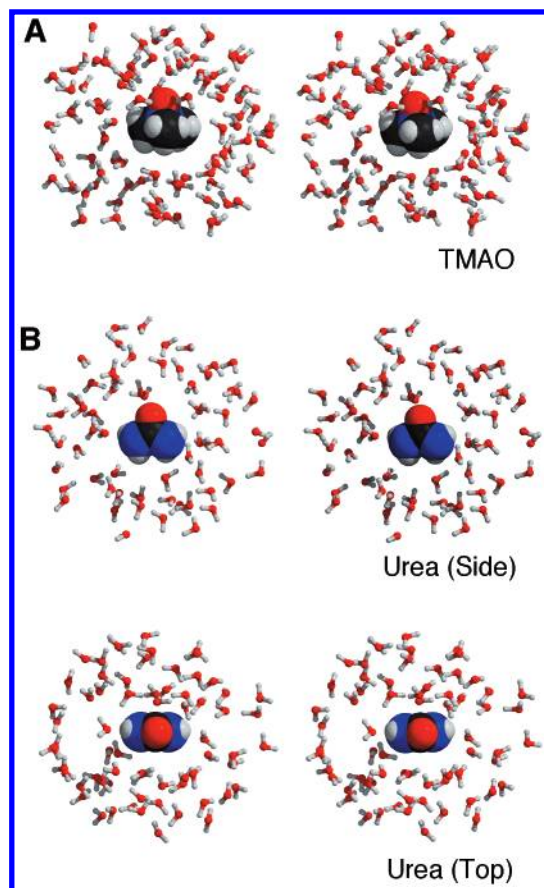


Figure 8. Representative stereoviews of molecular dynamics snapshots of TMAO (top) and urea (middle and bottom) with solvating water. Figures created with MOLSCRIPT⁴² and Raster3d.⁴³

Discussion

The Indirect Interaction between TMAO and the Amide Unit Is Dominant. Previous solubility studies have shown that the very unfavorable interaction between TMAO solution and the peptide backbone plays the major role in protein stabilization, while the slightly favorable interaction between TMAO solution and the apolar groups is relatively insignificant.¹⁹ The results shown here confirm this observation. The transfer ΔG for the amide unit from water to 1 M TMAO is large and positive (462 ± 60 J/mol) and that for one apolar hydrogen is small and negative (-15 ± 18 J/mol) (Table 2). The transfer ΔG for the peptide backbone ($-\text{HNCH}_2\text{CO}-$), 447 ± 63 J/mol, calculated from our results, is close to the value of Wang and Bolen (372 J/mol). Our estimate of transfer ΔG for the alanine side chain (with three apolar hydrogens) is -45 ± 54 J/mol, in reasonable agreement with their value of -54 J/mol.¹⁹

We showed previously that the transfer ΔG for the amide unit from water to 1 M urea is -54 ± 19 J/mol and that for one apolar hydrogen is -16 ± 4 J/mol (Table 2). Therefore, TMAO counteracts urea's denaturing effect because of the very different interactions with the amide unit. This effect is also reflected in terms of enthalpy and entropy; the large, positive transfer ΔG for the amide unit from water to TMAO consists of a positive enthalpy (2.0 ± 0.1 kJ/mol) and positive entropy (5.5 ± 0.5 J/mol·K), opposite in sign to the corresponding urea terms. The favorable transfer enthalpy and unfavorable transfer entropy of the amide unit from water to urea have been attributed to the hydrogen bonding between urea and the amide unit;²¹

therefore, it seems unlikely that TMAO will have a specific, direct interaction with the amide unit.

The cGG simulations can be used to supplement these observations. On the atomic level, the unfavorable interaction of the amide unit with TMAO can be seen in the hydrogen-bonding data, specifically the number of hydrogen bonds per water. Addition of 1 M TMAO to cGG did not enhance the number of hydrogen bonds per water in the hydration layer contrary to what is observed with the other solutes (Table 3, Figure 9). The data suggest that water around the amide portions of the peptide may face a penalty for participating in interactions with TMAO. In all cases, the number of hydrogen bonds per water was enhanced slightly in bulk water upon addition of 1 M TMAO. This effect reflects the enhanced water structure in the vicinity of the TMAO cosolvent molecules and TMAO's longer range spatial ordering of waters (Figure 7).

For the apolar groups, even though the transfer ΔG is the same in both TMAO and urea at 25° C, the origin of this favorable interaction is quite different. It is enthalpically driven in TMAO ($\Delta H_{\text{tr}} = -428 \pm 33$ J/mol, $\Delta S_{\text{tr}} = -1.4 \pm 0.1$ J/mol·K) but entropically driven in urea ($\Delta H_{\text{tr}} = 75 \pm 16$ J/mol, $\Delta S_{\text{tr}} = 0.30 \pm 0.04$ J/mol·K).²¹ The favorable transfer enthalpy of apolar groups into TMAO is reflected in the increased number of hydrogen bonds per water in the simulations of cAA relative to the pure water (Table 3). These data suggest that water-solvating apolar groups reorient to interact with TMAO instead of solute, as is illustrated in Figure 9. This enhancement of water structure favors hydrogen bonding and reduces entropy. The number of hydrogen bonds per water decreases when 1 M urea is added to cAA (Table 3, Figure 9). Because the solvation of apolar groups in urea is entropically driven, a reduction in hydrogen bonds is consistent with an increase in both the entropy and enthalpy changes. Also, the water around the cAA methyl groups is less ordered in 1 M urea than in pure water (Figure 7C), consistent with the increase in ΔS_{tr} . In contrast, water becomes more ordered around the methyl groups in the presence of TMAO (Figure 7C), which is consistent with the experimentally measured drop in entropy.

Lin and Timasheff¹⁵ have shown that at a 2:1 molar ratio of urea and TMAO, the effects of the urea/TMAO mixtures on RNase T1 is the algebraic sum of their individual effects. This rough additivity is also shown for the individual protein functional groups.¹⁹ For example, the transfer ΔG for the peptide backbone from water to 1 M TMAO + 2 M urea mixtures is roughly the algebraic sum of those in individual cosolvents. Our studies also show that the transfer ΔG 's for c(GG) and c(AA) are roughly additive in urea/TMAO mixtures (data not shown). Consequently, the counteraction of urea by TMAO might also include direct interactions between TMAO and urea and not only the independent TMAO and urea effects. The interaction between TMAO and urea in solution has been seen by the effect of TMAO on urea dilution heat (data not shown). The interaction is also seen in urea/TMAO cocrystals.³⁸ Contact data from the MD simulations suggest that TMAO and urea do indeed interact with one another. Table 4 shows that TMAO and urea interact more with each other than TMAO interacts with itself. In addition, TMAO's influence on water is more extensive than that of urea (Table 5). In fact, it takes about twice the amount

(38) Anthoni, U.; Christophersen, C.; Gajhede, M.; Nielsen, P. H. *Struct. Chem.* **1992**, 3, 121–128.

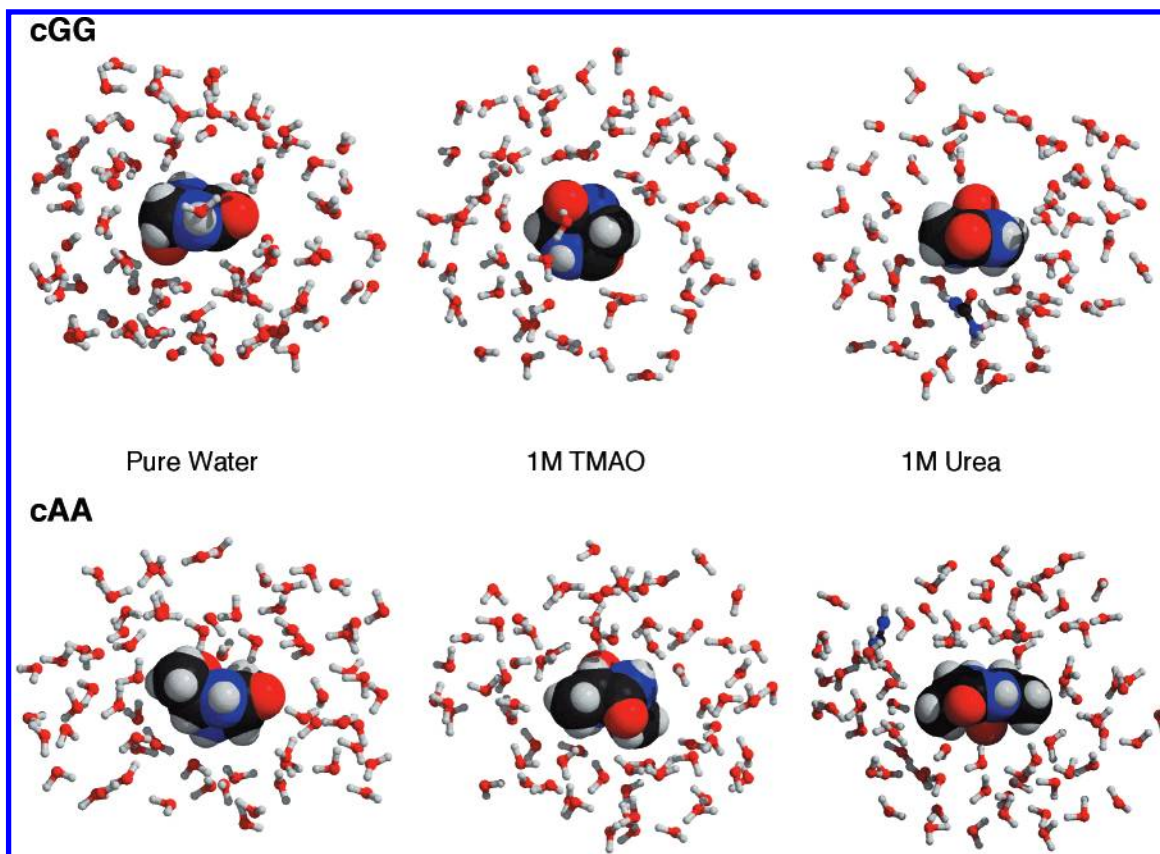


Figure 9. The environment around cGG and cAA in water, 1 M TMAO and 1 M urea is displayed for the 4-ns snapshots from the MD simulations. Figures created with MOLSCRIPT⁴² and Raster3d.⁴³

of urea to affect the same number of waters as TMAO (i.e. 2 M urea is comparable to 1 M TMAO, Table 5).

TMAO Interacts Indirectly with the Protein Functional Groups by Enhancing Water Structure. Protein stabilization by TMAO has been explained by a preferential exclusion mechanism,¹⁵ which suggests that the stabilizing osmolyte is excluded from the protein surface such that TMAO does not interact directly with proteins. Bolen and co-workers¹⁹ have shown that the interaction of TMAO with the peptide backbone is very unfavorable and dominates the stabilization, consistent with the preferential exclusion mechanism. Further, Collins and Washabaugh proposed that kosmotropes (water-structure makers, i.e., TMAO) interact more strongly with their hydration layer than chaotropes (urea).^{44,45} In the MD simulations of 1 M TMAO solutions, TMAO rarely interacted with cGG and cAA (Table 4), but TMAO decreased water diffusion and increased water hydrogen bonding (Table 3). The opposite was observed with urea (Table 3). When contacts or hydrogen bonds did occur, they were very transient. These observations imply that TMAO affects protein stability indirectly by affecting water structure, at least at these low concentrations.

Other experimental and computational studies also indicate that TMAO enhances water structure. Infrared spectroscopic

studies show that the bond-stretching frequency of the water O—H bond is lower in TMAO solution than in pure water, indicating that the water hydrogen bonds are stronger.⁴⁶ Ab initio calculations and molecular dynamics simulation²⁰ also show that water molecules are more tightly coordinated around TMAO than around *tert*-butyl alcohol (TBA), an isosteric molecule that is a denaturant. The simulations described here support these findings. Water is tightly coordinated to TMAO, and the hydrogen bonds between them last 7 times longer, on average, than water—water hydrogen bonds (Figure 8 and Table 3). In addition, the water—water hydrogen bonding distances of the hydration shell shift to lower values in the presence of TMAO (Figure 10), that is, TMAO increases the strength of water—water hydrogen bonds.

Further analysis of water structure in the MD simulations provides insight into the orientation of water around solutes. The angular orientation data in Figure 7 can be interpreted in terms of the three-dimensional structure of TMAO and urea and the resulting perturbation on solvation water. TMAO and urea have similar effective lengths and electronegative oxygen atoms, suggesting there should be some angular maxima in common. This is the case with respect to the 5 Å maximum (Figures 7 and 8), where water in the first shell is somewhat flattened around the nonpolar portions of TMAO and around the amide hydrogens of urea. Both solutes have similar water orientation about their oxygen atom (Figures 7 and 8). However, there are also differences between TMAO and urea that can be explained based on their structures. TMAO is semispherically

(39) Habermann, S. M.; Murphy, K. P. *Protein Sci.* **1996**, *5*, 1229–1239.

(40) Laidig, K. E.; Daggett, V. *J. Phys. Chem.* **1996**, *100*, 5616–5619.

(41) Muller, N. *Acc. Chem. Res.* **1990**, *23*, 28–33.

(42) Kraulis, P. J. *J. Appl. Crystallogr.* **1991**, *24*, 946–950.

(43) Merritt, E. A.; Bacon, D. J. *Macromol. Crystallogr. Part B* **1997**, *277*, 505–524.

(44) Collins, K. D.; Washabaugh, W. M. *Q. Rev. Biophys.* **1985**, *18*, 323–422.

(45) Washabaugh, W. M.; Collins, K. D. *J. Biol. Chem.* **1986**, *261*, 2477–2485.

(46) Sharp, K. A.; Madan, B.; Manas, E.; Vanderkooi, J. M. *J. Chem. Phys.* **2001**, *114*, 1791–1796.

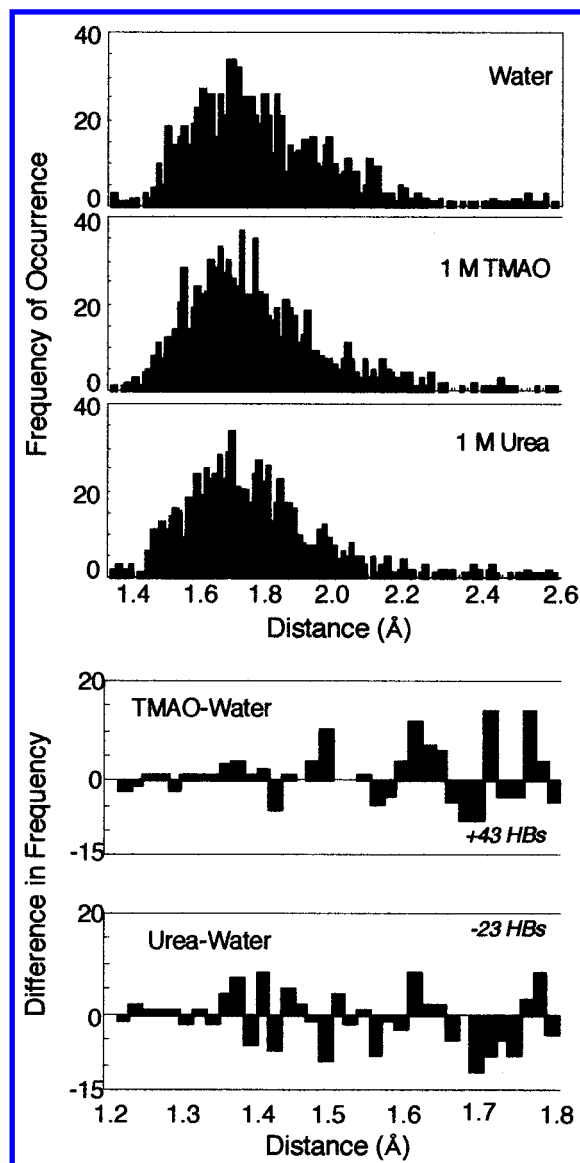


Figure 10. Histograms of hydrogen bond distances in the hydration shells around water in pure water, 1 M TMAO, and 1 M urea. Similar distributions are obtained for the bulk. Hydrogen bonds are defined as a hydrogen atom within 2.6 Å of an acceptor atom with an acceptor–H–donor angle less than 35° from linearity. Differences in frequency of occurrence are shown for tight hydrogen bonds (1.2–1.8 Å). Relative to pure water, 1 M TMAO gains 43 new hydrogen bonds in the 1.2–1.8 Å portion of the distribution, compared with a loss of 23 hydrogen bonds in 1 M urea.

symmetric, such that it presents a more uniform surface to the solvating water molecules than urea (Figure 8). Water ordered around TMAO produces a structure with a distinct void (~4 Å) between the methyl groups and surrounding waters that gradually decreases to clusters of tight waters around the oxygen of TMAO (Figure 8). This path can be followed from all sides of TMAO. The effect on the solvating waters seems to be more favorable in TMAO than urea as a result of its unique symmetry, and the induced order favors water–water interactions quite distant from TMAO (Table 3, Figure 7).

While urea has molecular symmetry about its carbonyl carbon, it does not present a spherically symmetric surface to hydrating water and therefore more asymmetry and disorder is imparted to the water in the “sphere of influence” of urea relative to that of TMAO. Water-solvating urea has the appearance of

a two-sided dome when viewed through the plane of the molecule (Figure 8). Water forms an arch as it hydrogen bonds to each polar end of the molecule. The top of the arch from the carbon to water is about 4 Å high (Figure 8).

The transfer energetics of protein functional groups from water into TMAO solution presented here can be rationalized by the ability of TMAO to enhance water structure. The transfer of an amide unit from water into TMAO solution is accompanied by a large and positive ΔH and a positive ΔS . The MD simulations suggest, as a first approximation, that the interactions between water and the amide unit are approximately the same in pure water and 1 M TMAO. Also, there is little difference in water structure and hydrogen bonding around cGG in pure water and 1 M TMAO. However, TMAO leads to stronger water–water hydrogen bonds in the absence of peptide. So, these water hydrogen bonds are somewhat disrupted and weakened upon the addition of peptide, which leads to a positive ΔH and ΔS of transfer.

When a protein unfolds, hydrogen bonds between amide groups in the protein interior are broken and replaced with hydrogen bonds with water. This exchange requires that some water–water hydrogen bonds are also broken. The breaking of protein and water hydrogen bonds is enthalpically unfavorable and the overall ΔH° associated with the loss of amide–amide hydrogen bonds upon unfolding is unfavorable,³⁹ that is, hydrogen bonds are enthalpically stabilizing. The unfavorable enthalpy of transferring hydrogen-bonding groups to TMAO solution relative to water enhances the enthalpic stabilization of proteins by hydrogen bonds.

The favorable transfer ΔG of the apolar groups to TMAO is intriguing because it is nearly equivalent to that for transfer from water to 1 M urea.²¹ However, as noted above, the ΔH and ΔS of transfer for the two processes are of opposite signs. The unfavorable ΔH and favorable ΔS of transferring apolar groups from water to urea solution has been interpreted as a decrease in the hydrophobic effect arising from the replacement of some water molecules in the hydrophobic solvation shell by urea.^{21,40–41} In the transfer of hydrophobic groups to TMAO solution, the favorable ΔG of transfer arises from a favorable ΔH despite an unfavorable ΔS . These results can also be rationalized in terms of TMAO’s ability to enhance water structure. The number of hydrogen bonds per water molecule is enhanced around the cAA methyl groups in the presence of TMAO (Table 3), and the water is more ordered (Figure 7C) compared with cAA in pure water. These findings are consistent with a drop in both ΔH and ΔS . In contrast, the hydrogen bonding is compromised slightly in urea and the water is less ordered, consistent with an increase in both ΔH and ΔS .

Conclusions

In summary, our thermodynamic studies have shown that the unfavorable interaction between TMAO and the amide unit is the dominant factor in the ability of TMAO to stabilize proteins, consistent with previous studies.¹⁹ Furthermore, we have demonstrated that the counteraction of the urea effects by TMAO occurs not only at the level of free energy but also in terms of enthalpy and entropy. The results can best be rationalized on the basis of the ability of TMAO to enhance water structure as seen in the MD simulations via an increase in water–water hydrogen bonds, stronger hydrogen bonds, and

greater spatial ordering of the waters. In contrast, the addition of urea weakens water–water interactions. Consequently, it is likely that low concentrations of TMAO stabilize proteins and offset the effects of urea by interacting indirectly with protein functional groups through enhancement of water structure.

Acknowledgment. We thank Drs. Wayne Bolen, Kim Sharp, Andrew Robertson, Darwin Alonso, and Margarida Bastos for critical comments and helpful discussions. We thank Keith Laidig for performing some of the early urea simulations. We

also thank Drs. Kim Sharp and Jane Vanderkooi for sharing their results prior to publication, and Drs. Wayne Bolen and Mathew Auton for providing density data for the TMAO solutions. This work was supported by the National Science Foundation (MCB-9808073 to K.M.), the Office of Naval Research (N00014-99-1-0245 to V.D.) and a NIGMS National Research Service Award (GM-07750 to B.J.B.).

JA004206B